

## TURNING UP THE HEAT ON ‘OUMUAMUA

JOHN C. FORBES AND ABRAHAM LOEB

Astronomy Department, Harvard University, 60 Garden St., Cambridge MA 02138, USA;  
john.forbes@cfa.harvard.edu, aloeb@cfa.harvard.edu

*Draft version January 4, 2019*

### ABSTRACT

We explore what may be learned by close encounters between extrasolar minor bodies like ‘Oumuamua and the Sun. These encounters may yield strong constraints on the bulk composition and possible origin of ‘Oumuamua-like objects. We find that such objects collide with the Sun once every 30 years, while about 2 pass within the orbit of Mercury each year. We identify preferred orientations for the orbits of extrasolar objects and point out known Solar System bodies with these orientations. We conclude using a simple Bayesian analysis that about one of these objects is extrasolar in origin, even if we cannot tell which.

*Keywords:* comets: general, comets: individual (C/2012 S1 ISON, C/2011 W3 Lovejoy, C/2011 N3 SOHO, 96P/Machholz 1), minor planets, asteroids: individual (‘Oumuamua A/2017 U1)

### 1. INTRODUCTION

The detection of the interstellar object ‘Oumuamua on October 19, 2017 (Meech et al. 2017) was a surprise. Previous studies predicting the number density of interstellar comets in the galaxy were pessimistic that they would be detected even in the next generation of transient surveys (Moro-Martín et al. 2009). The detection of even a single object like ‘Oumuamua immediately implied a vast abundance of interstellar objects (Laughlin & Batygin 2017; Do et al. 2018), though their exact number density and size distribution remain uncertain.

Since its discovery, the physical nature of ‘Oumuamua has been debated, with different lines of evidence pointing to an asteroidal composition, while others point to a cometary origin. A priori ‘Oumuamua was expected to be an interstellar comet because solar systems likely have many icy bodies loosely bound in their outskirts. However, this picture was called into question when ‘Oumuamua showed no direct sign of cometary activity while observed in the solar system: no tails, and no dust (Micheli et al. 2018) or carbon-based molecules (Trilling et al. 2018). These facts pointed away from a cometary origin, but are far from definitive. Seligman & Laughlin (2018) have argued that a comparatively thin layer of material could have insulated ‘Oumuamua’s interior and prevented the traditional outgassing and brightening expected of comets.

Recently Micheli et al. (2018) discovered that the observed positions of ‘Oumuamua on the sky as it departs the solar system were highly significantly inconsistent with a purely hyperbolic orbit expected of purely gravitational forces. Non-gravitational accelerations are not uncommon among solar system comets (Rafikov 2018a), and in fact the level of non-gravitational acceleration is within the range of values observed in the solar system. The favored explanation presented in Micheli et al. (2018) is that there is directed outgassing, i.e. a jet, causing the non-gravitational acceleration, but because of unusual dust properties and carbon abundance, no dust (Micheli et al. 2018) or gas (Trilling et al. 2018) from ‘Oumuamua has been observed. Rafikov (2018b) argues that a cometary jet of this sort should generically

cause a rapid evolution in the spin of ‘Oumuamua that was not observed, unless there is extreme fine tuning of the lever arm of the jet’s torque. Another possibility is that the standard estimates for ‘Oumuamua’s albedo (both its magnitude and isotropy over the surface) are mistaken, and the object is not as elongated as naively inferred from the lightcurve. Another related possibility is that ‘Oumuamua is sufficiently reflective and low in mass, consistent with its lack of detection in Spitzer (Trilling et al. 2018), that radiation pressure may affect its orbit (Bialy & Loeb 2018; Sekanina & Kracht 2018).

As the debate continues between asteroidal and cometary interpretations, it remains unclear if any firm conclusions can be reached as ‘Oumuamua itself has rapidly faded from view on its way out of the Solar System. Hein et al. (2017) has proposed a technically challenging mission that could use a gravitational assist from the sun to catch up to ‘Oumuamua for a flyby or in-situ measurement. More practically, Seligman & Laughlin (2018) have proposed preparing now for the likely future discovery of an interstellar object with a favorable orbit easily reachable with available rocketry. This would be particularly feasible for interstellar objects that were trapped in the Solar System by the gravitational “fishing net” of Jupiter and the Sun which may be identified through anomalous oxygen isotope ratios (Lingam & Loeb 2018) or their high inclination orbits (Siraj & Loeb 2018).

While in-situ exploration would no doubt settle the question of interstellar objects’ compositions and yield other interesting discoveries, there may be a cheaper alternative. In this work we explore what may be learned by interstellar objects that happen to pass close to the Sun. In section 2 we discuss the expected rate and orbital parameters of such objects, and in section 3 we comment on the compositional constraints that may be obtained in these events.

### 2. RATES AND ORBITS

The rate of encounters between the solar system and interstellar objects of number density  $n$  moving with typ-

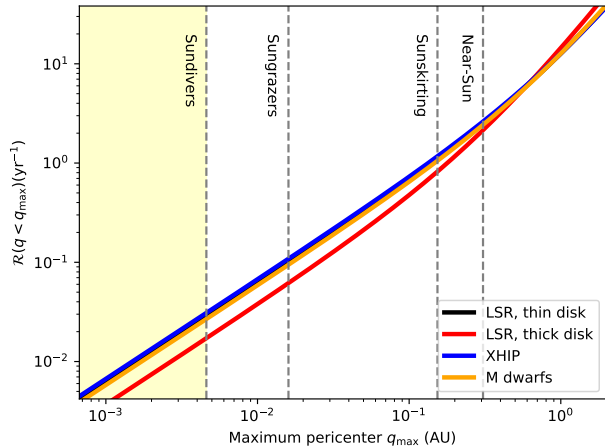


**Figure 1.** Expected rates per year of interstellar objects with perihelion values less than  $q_{\max}$ . Each line shows a different assumption about the velocity distribution of interstellar objects - see Table 1 and text for details. Vertical lines indicate different categories of near-Sun objects, with objects that directly impact the Sun (Sundivers) shaded yellow.

ical velocity  $v$  is

$$\mathcal{R} = n\sigma v, \quad (1)$$

where the cross-section  $\sigma$  is dependent on both the velocity of the object far from the Sun and the maximum pericenter distance of interest  $q_{\max}$ ,

$$\sigma = \pi q_{\max}^2 \left( 1 + \frac{2GM_{\odot}}{q_{\max}v^2} \right). \quad (2)$$

Here the first term is the geometrical cross-section, and the second accounts for gravitational focusing.

The rate from Equation (1) can be generalized to account for the full velocity distribution, which we refer to as  $f(\vec{v})$ . In this case

$$\mathcal{R}(q < q_{\max}) = \int \int \int f(\vec{v}) \sigma(|\vec{v}|, q_{\max}) n |\vec{v}| d^3\vec{v}, \quad (3)$$

where the integrations are carried out over all possible values of the velocity vector. The distribution function of interstellar objects is tied to the velocity distribution of stars in the solar neighborhood, since the large abundance of interstellar objects inferred by ‘Oumuamua’s detection necessitate contributions from most stars (Do et al. 2018). The velocity distribution of stars in the solar neighborhood is roughly Gaussian, though there is a correlation between stellar age and velocity dispersion (e.g. Nordström et al. 2004). The vertical velocity dispersion is smaller than the in-plane motion, and the velocity distribution is not centered on zero, but related to the Solar System’s motion with respect to nearby stars. As discussed by Mamajek (2017), ‘Oumuamua’s inferred velocity as it entered the Solar System was not far from the canonical velocity of the Local Standard of Rest (hereafter LSR), namely the inverse of the Solar motion in the frame of the LSR,  $U, V, W = -7, -11, -10$  km/s (Bland-Hawthorn & Gerhard 2016). Its inferred velocity was even closer to the mean velocity of the Reid et al. (2002) M dwarf sample and the XHIP sample of nearby stars (Anderson & Francis 2012). These velocity distributions

**Table 1**  
Plausible Velocity Distributions (units of  $\text{km s}^{-1}$ )

	U	V	W	$\sigma_U$	$\sigma_V$	$\sigma_W$
LSR, thin disk	-10	-11	-7	35	25	25
LSR, thick disk	-10	-11	-7	50	50	50
XHIP	-10.5	-18	-8.4	33	24	17
M dwarfs	-9.7	-22.4	-8.9	37.9	26.1	20.5

are summarized in Table 1, though we note that the velocity distribution of nearby stars contains substantial substructure (e.g. Trick et al. 2018), so this Gaussian model of  $f(\vec{v})$  is an approximation. Our fiducial estimates will assume the first line of the table, namely a velocity centered on the LSR with a dispersion appropriate for the thin disk at an age of  $\sim 10$  Gyr (Bland-Hawthorn & Gerhard 2016).

Figure 1 shows the cumulative rate of encounters between interstellar objects and the Sun as a function of pericenter distance, with vertical dashed lines indicating various classes of Sungrazing comets as suggested in the review by Jones et al. (2018). The boundaries in pericenter correspond to objects that hit the Sun (Sundivers), pass within the fluid tidal radius (Sungrazers), pass within half the semi-major axis of Mercury (Sunskirters), and pass within Mercury’s orbit (near-Sun). The different colored lines show rates assuming different plausible velocity distributions,  $f(\vec{v})$ . While there is some difference, the uncertainty is dominated by the estimate of the interstellar density, which is based on the detection of a single object.

Assuming the Do et al. (2018) estimate for the density of interstellar objects leads to rates of close encounters with the Sun between a few per year and about 1 per 30 years, depending on the exact pericenter distance. This raises a few interesting prospects, namely *the possibility that one or more near-Sun comets detected in the past few decades was interstellar in origin, and the high likelihood that many interstellar objects will have observable close encounters with the Sun in the coming years.*

To address these possibilities, we set out to determine the expected distribution of the orbits of interstellar objects. We do so via a Monte Carlo method. In particular, for a given value of  $q_{\max}$ , we first draw  $N$  values of the velocity vector from its distribution  $f(\vec{v}_i)$  where  $i = 1, \dots, N$ . Each of these samples is weighted by  $w_i = \sigma(|\vec{v}_i|, q_{\max}) |\vec{v}_i|$ . Then  $M$  samples are drawn from this weighted distribution, i.e. for each draw (which we shall index by  $j$ ) a given  $\vec{v}_i$  is chosen with probability  $w_i / \sum_{i=1}^N w_i$ . We use  $N = 2 \times 10^5$  and  $M = 1 \times 10^5$  throughout this work. Having specified the object’s velocity far from the solar system  $\vec{v}_j$ , we now specify a spatial position to fully determine its orbit.

First, we determine the object’s location in cylindrical coordinates with the positive axis of symmetry pointed in the direction of  $-\vec{v}_j$ . The object’s location along this axis is taken to be an arbitrarily large number ( $10^5$  AU). Within the plane specified by this ‘height’ above the sun, a coordinate is drawn at random from a disk extending out to a maximum impact parameter

$$b_{\max} = q_{\max} \sqrt{1 + 2GM_{\odot}/(q_{\max}v^2)}, \quad (4)$$

i.e.  $\sqrt{\sigma/\pi}$ . This entails drawing a value of the cylindrical coordinate  $\theta$  uniformly from 0 to  $2\pi$ , and the impact

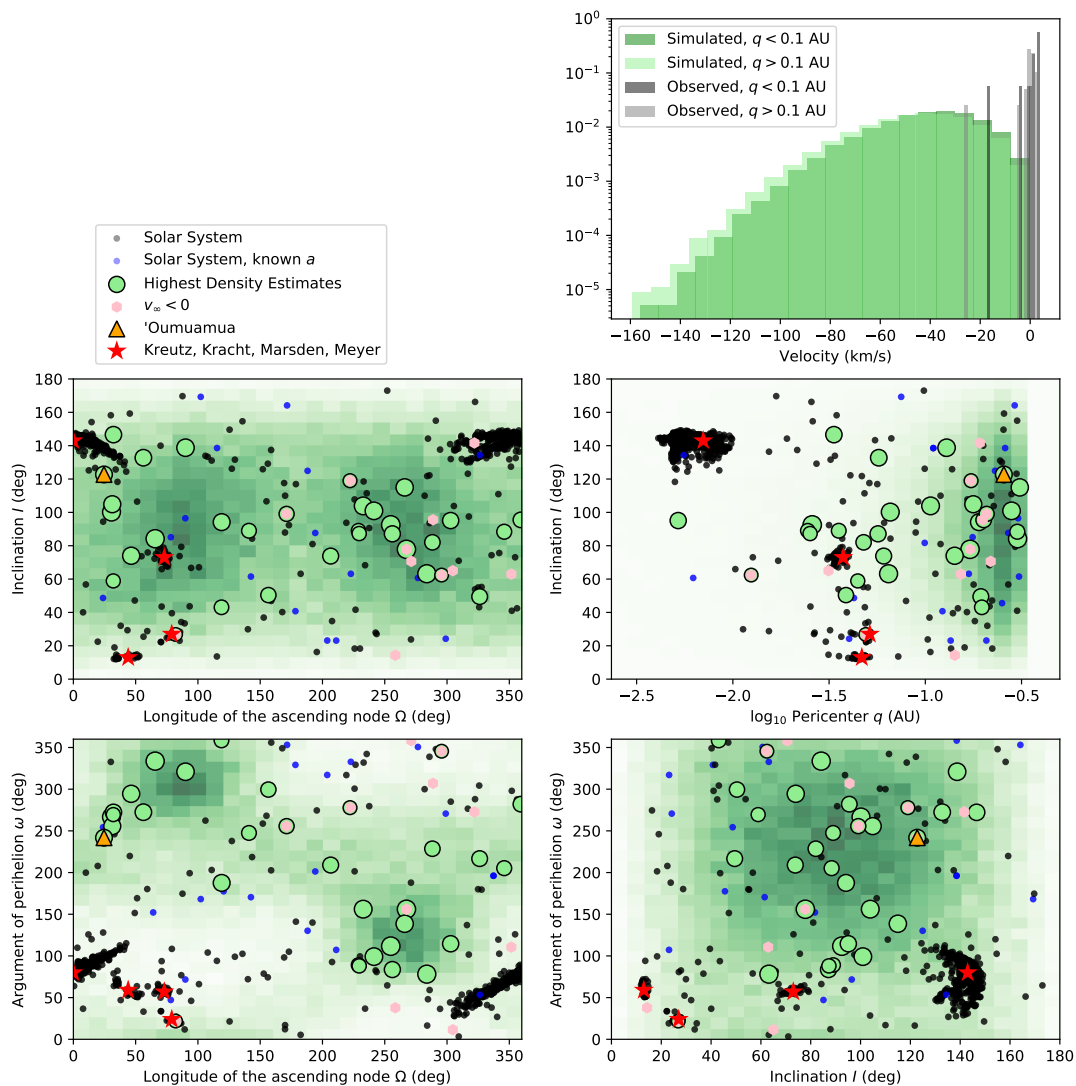


**Figure 2.** Orbital Parameters. The bottom four panels show orbital elements for solar system bodies (small black or blue dots). Typical values for known Sungrazing or Sunskirting groups are marked as red stars, and ‘Oumuamua is shown as an orange triangle. The green histogram shows the distribution of simulated interstellar comets assuming a velocity distribution far from the Sun centered on the LSR velocity with velocity dispersions appropriate for the thin disk of the Milky Way. Green circles are Solar System objects that lie within the greatest density points as estimated by the 3D histogram in  $\Omega$ ,  $\omega$ , and  $I$ . The upper right panel shows the distributions of velocities  $v_\infty$ , with negative values meaning objects with hyperbolic orbits. Objects with  $v_\infty < -1$  km/s are highlighted in pink in the lower four panels.

parameter is set by  $b = b_{\max} \sqrt{u}$ , where  $u$  is drawn from a uniform distribution between 0 and 1. These coordinates are then transformed into galactic Cartesian coordinates, and finally both the position and velocity vectors are transformed from galactic to solar system cartesian coordinates via the rotation matrix defined in the Gaia DR1 documentation.<sup>1</sup> Once transformed into the solar system Cartesian coordinates, i.e. the International Celestial Reference System (ICRS), we compute the standard orbital elements of these orbits, namely the semi-major axis, eccentricity, inclination, longitude of the ascending node, and argument of perihelion  $a$ ,  $e$ ,  $i$ ,  $\Omega$ , and  $\omega$ , respectively.

Figure 2 shows the distribution of these simulated orbits in the green histogram. For comparison we show the

sample of comets and asteroids from the JPL small-body database<sup>2</sup> with pericenter  $q < 0.3$  AU (to focus on near-sun objects), and with orbits determined to be parabolic or hyperbolic<sup>3</sup>.

The vast majority of known small Solar System bodies in this regime belong to the Kreutz group of Sungrazing comets (Kreutz 1888). This and other groups are clearly visible as clusters in Figure 2, with orbital parameters of each from Jones et al. (2018) marked as red stars. These groups are each likely the result of a large progenitor body that has since fragmented. These groups are well-separated from the expected distribution of interstellar objects, though this is sensitive to assumptions about

<sup>2</sup> [https://ssd.jpl.nasa.gov/sbdb\\_query.cgi](https://ssd.jpl.nasa.gov/sbdb_query.cgi)

<sup>3</sup> Queries were limited to be members of Parabolic Asteroid, Hyperbolic Asteroid, Asteroid (other), Hyperbolic Comet, Parabolic Comet, or Comet (other)

<sup>1</sup> [https://gea.esac.esa.int/archive/documentation/GDR1/pdf/GaiaDR1\\_documentation\\_D.0.pdf](https://gea.esac.esa.int/archive/documentation/GDR1/pdf/GaiaDR1_documentation_D.0.pdf) subsection 3.1.7.1.1

$f(\vec{v})$ . ‘Oumuamua itself (shown as the orange triangle) is not in the peak of the distribution, but is within the expected range. To quantify this, we estimate the probability density over  $\Omega$ ,  $\omega$ , and  $I$  by filling a histogram with the  $M$  sample orbits (the same histogram shown in Figure 2). The resulting probability distribution  $f(\Omega, \omega, I)$  is normalized so that

$$\int_0^{2\pi} \int_0^{2\pi} \int_0^\pi f(\Omega, \omega, I) d\Omega d\omega dI = 1, \quad (5)$$

We highlight known small solar system bodies whose orbital elements give them values of  $f(\Omega, \omega, I)$  greater than two thirds of ‘Oumuamua’s value of  $f$ , as light green circles in Figure 2, and in Table 2. In addition to comets with large values of  $f(\Omega, \omega, I)$ , we also include two near-Sun comets with  $v_\infty < -1$  km/s, where  $v_\infty = \text{sign}(a)\sqrt{GM_\odot/|a|}$ .

We also estimate the probability that any one is extra-solar based purely on the orientation of its orbit (obviously the energy of the orbit would be a stronger indicator, but this is more difficult to measure). We apply Bayes’ Theorem,

$$P(ES|\vec{\phi}_i) = \frac{f(\vec{\phi}_i|ES)P(ES)}{f(\vec{\phi}_i|ES)P(ES) + f_{\text{ISO}}(\vec{\phi}_i|\text{LPC})P(\text{LPC})}, \quad (6)$$

where the angles have been abbreviated  $\vec{\phi}_i = (\Omega_i, \omega_i, I_i)$ ,  $P(ES)$  is the prior probability that a given object is extra-solar,  $P(\text{LPC})$  is the prior probability that a given object is a long-period comet (hereafter LPC), and  $f_{\text{ISO}}$  is constructed in the same way as  $f(\vec{\phi})$ , except that the velocity distribution from which the simulated comets are drawn is centered at zero and isotropic with  $\sigma_U = \sigma_V = \sigma_W = 1$  km/s.

To estimate  $P(ES)$ , we compare the rate of extra-solar objects (Equation 3) to the observed rate of dynamically new comets. For now we shall proceed under the naive assumption that the two size distributions are similar leaving  $P(ES)$  independent of size. ‘Oumuamua has an absolute magnitude of  $H_{10} \approx 22.08$  (e.g. Bolin et al. 2018). If the cumulative number density of comets is proportional to  $10^{\alpha H_{10}}$  with  $\alpha \approx 0.28$  (Hughes 1988; Weissman & Lowry 2001), then extrapolating the flux of comets of  $\sim 1 \text{ yr}^{-1}$  within 5 AU for  $H_{10} < 7$  to ‘Oumuamua-sized objects, we find a rate of about  $1.7 \times 10^4 \text{ yr}^{-1}$ , though the rate may be closer to  $10^3 \text{ yr}^{-1}$  if the slope is shallower, with  $\alpha = 0.2$  as per Fernández & Sosa (2012). For different assumptions about  $f(\vec{v})$  the expected rate of ‘Oumuamua-sized objects with pericenters  $q < 5 \text{ AU}$  is about  $200 \text{ yr}^{-1}$ , keeping in mind the order of magnitude uncertainty from the background density being estimated from a single object. This implies that  $P(ES)$  should be between 0.01 and 0.2.

Both interstellar objects and LPCs are subject to gravitational focusing, but the lower velocity of the LPCs enhances their rate by an additional factor of 2. Since LPCs also brighten as they approach pericenter, there may be a bias in composition. If extra-solar objects are rocky or have a layer of material protecting more volatile-rich interiors, they may be harder to discover than LPCs, in which case the range of  $P(ES)$  estimated purely on the rates may be more like an upper limit. We therefore con-

servatively adopt  $P(ES) \lesssim 0.01$  as the plausible range for the prior, with lower values corresponding to rockier compositions, lower intrinsic rates, or steeper faint-end brightness distributions for LPCs. Table 2 includes estimates of the posterior probability that a given object is extra-solar in origin  $p(ES|\vec{\phi})$  under the assumption that  $P(ES) = 0.01$  for all objects.

### 3. CLOSE ENCOUNTERS WITH THE SUN

There is a long history of the spectroscopic and narrow-band study of cometary tails with ground-based telescopes (A’Hearn et al. 1995; Fink 2009; Langland-Shula & Smith 2011). Generally these studies are able to classify comets into different groups depending on the inferred production rates of  $\text{H}_2\text{O}$ ,  $\text{C}_2$ , CN, and  $\text{NH}_2$  as well as dynamical properties, which likely reflect formation in different parts of the protoplanetary disk (Levison 1996). Two comets, 96P/Machholz 1 (Schleicher 2008; Langland-Shula & Smith 2007) and Yanaka (1998r) have been shown to have highly depleted CN and  $\text{C}_2$  relative to water, leading some to conjecture that they are interstellar in origin (de la Fuente Marcos et al. 2018). The promise of using close encounters with the sun to learn about extrasolar small bodies is that the sun has the ability to disrupt even large cometary nuclei via its intense radiation, sublimating not just surface volatiles but even silicates and iron. In principle this exposes the interiors of these objects to remote spectroscopy, which could place strong constraints on the composition of these objects.

This has been done a few times, notably with the Atmospheric Imaging Assembly (AIA Lemen et al. 2012), an EUV imager aboard the Solar Dynamics Observatory (SDO). AIA successfully observed comet C/2011 N3 (SOHO) in the process of being destroyed (Schrijver et al. 2012), and observations of comet C/2011 W3 Lovejoy were used as a probe of magnetic structure in the solar corona (Downs et al. 2013; Raymond et al. 2014). Lines of variously-ionized iron, oxygen, and carbon happen to lie in the AIA bands which are centered around high-ionization lines of iron common in the solar corona (e.g. Bryans & Pesnell 2012). As the comet loses mass, the iron and oxygen in the tail are ionized by the corona and emit light in the different AIA bands. This process is nontrivial to model, and occurs over only about a minute. These measurements therefore yield only broad indications of the comet’s composition. The observations tend to be well-fit by a model with standard cometary abundances (Bryans & Pesnell 2012; Pesnell & Bryans 2014). Observations by the Ultraviolet Coronagraph Spectrometer (UVCS) (Kohl et al. 1995) aboard the Solar and Heliospheric Observatory (SOHO) have also been used to constrain the abundance of silicates sublimating from C/2011 W3 (Raymond et al. 2018), though UVCS is no longer operational.

Directed observations by the AIA for the well-studied comet C/2012 S1 (ISON) yielded no detections, which serves as a cautionary tale for the study of sungrazing comets with this method; likely the nucleus lost so much mass that by the time it reached the AIA field of view its surface area, and hence volatile production rate, had decreased below the detectable level (Bryans & Pesnell 2016) - this size was only modestly smaller than ‘Oumuamua’s. Another telescope with the potential to observe

**Table 2**  
Known comets that line up well with the expected properties of interstellar objects

Full Name	q (AU)	e	I (deg)	$\Omega$ (deg)	$\omega$ (deg)	$v_\infty$ (km/s) <sup>a</sup>	$4\pi^3 f(\vec{\phi})$	$p(ES \vec{\phi})^b$
C/1865 B1 (Great southern comet)	0.03	1.0	92.49	254.83	111.72	-	4.17	0.0338
C/2006 P1 (McNaught)	0.17	1.0000190685	77.84	267.41	155.97	-0.31	3.43	0.026
C/2011 L4 (PANSTARRS)	0.3	1.00003268452	84.21	65.67	333.65	-0.31	3.06	0.0192
C/1689 X1	0.06	1.0	63.2	283.75	78.13	-	2.87	0.0181
C/1970 B1 (Daido-Fujikawa)	0.07	1.0	100.18	30.61	266.65	-	2.69	0.0131
C/1665 F1	0.11	1.0	103.89	232.7	156.09	-	2.69	0.0205
C/1677 H1	0.28	1.0	100.93	241.32	99.16	-	2.69	0.0238
C/1910 A1 (Great January comet)	0.13	0.999995	138.78	90.04	320.91	0.19	2.59	0.0535
C/1884 A1 (Ross)	0.31	1.0	114.98	265.99	138.6	-	2.5	0.0222
C/1851 U1 (Brorsen)	0.14	1.0	73.99	46.43	294.45	-	2.5	0.0265
C/1577 V1	0.18	1.0	104.88	31.24	255.67	-	2.41	0.0198
C/2002 X5 (Kudo-Fujikawa)	0.19	0.999842855646	94.15	119.07	187.58	0.86	2.32	0.0131
'Oumuamua (A/2017 U1)	0.26	1.2011337961	122.74	24.6	241.81	-26.41	2.22	-
C/1997 B4 (SOHO)	0.06	1.0	132.78	56.2	272.4	-	2.04	0.0129
C/2000 J2 (SOHO)	0.03	1.0	146.61	32.19	272.21	-	2.04	0.0241
C/2001 N1 (SOHO)	0.01	1.0	95.09	302.92	114.59	-	2.04	0.0137
C/2000 Q1 (SOHO)	0.06	1.0	87.14	256.11	83.66	-	1.94	0.0131
C/1882 F1 (Wells)	0.06	0.999993648982	73.8	206.59	208.98	0.3	1.85	0.0125
C/1945 W1 (Friend-Peltier)	0.19	1.0	49.48	326.2	216.71	-	1.85	0.0125
C/1859 G1 (Tempel)	0.2	1.0	95.49	359.31	282.0	-	1.76	0.0126
C/2007 M8 (SOHO)	0.05	1.0	82.04	288.26	228.58	-	1.76	0.0091
C/2005 Q6 (SOHO)	0.04	1.0	50.4	156.59	299.54	-	1.76	0.0209
C/2017 S3 (PANSTARRS)	0.21	1.00476984465	99.1	171.2	255.67	-4.51	1.76	0.0086
C/1989 W1 (Aarseth-Brewington)	0.3	1.00009317367	88.39	345.91	205.26	-0.52	1.67	0.0128
C/2005 M3 (SOHO)	0.04	1.0	88.99	140.98	247.5	-	1.67	0.01
C/1975 V1-A (West)	0.2	0.999971	43.07	118.92	358.43	0.36	1.57	0.0187
C/2000 Y7 (SOHO)	0.02	1.0	89.02	228.93	89.13	-	1.57	0.0094
C/2000 Y6 (SOHO)	0.03	1.0	87.3	229.47	88.03	-	1.57	0.0094
C/1874 D1 (Winnecke)	0.04	1.0	58.89	32.05	269.51	-	1.57	0.0187
C/1853 R1 (Bruhns)	0.17	1.000664	119.0	222.12	277.84	-1.85	1.3	0.0074
C/2012 S1 (ISON)	0.01	1.00020100383	62.4	295.65	345.53	-3.78	1.11	0.0052

<sup>a</sup>Based purely on instantaneous estimates of  $a$ ; comets with  $v_\infty < 0$  may in fact be bound to the Solar System.

<sup>b</sup>Assuming a prior  $P(ES) = 0.01$

sungrazing comets is the forthcoming Daniel K. Inoue Solar Telescope<sup>4</sup> (DKIST). DKIST will observe the sun at high spatial and temporal resolution, and is equipped with multiple spectro-polarimeters. Although its field of view is comparatively small, detection of sungrazing comets sufficiently early will likely enable the telescope to be pointed away from its usual target, as the AIA did to observe C/2012 S1. DKIST's capabilities in this realm may be limited by its lack of a coronagraph (Jones et al. 2018), but its unprecedented sensitivity and resolution may yield interesting discoveries.

These examples illustrate the value of obtaining spectral or narrow band imaging from Sungrazing comets in the UV, but also illustrate some of the difficulties of doing so. The relatively small number of observations is the result of the challenge of identifying these comets sufficiently far in advance. Even Kreutz group comets, for which the approximate rate and orbital parameters are reasonably well-known, have rarely been identified in ground-based surveys (Knight et al. 2010; Ye et al. 2014). Undoubtedly this will change with the Large Synoptic Survey Telescope (LSST Schwamb et al. 2018), and we can expect the detections of interstellar objects and Sungrazing comets to increase dramatically. Direct impacts with the sun, while rare, may also yield substantial information as the comet is rapidly destroyed (Brown et al. 2011, 2015).

<sup>4</sup> <https://dkist.nso.edu/>

#### 4. CONCLUSION

We have examined the rate and orientation of orbits for extrasolar comets that have perihelion distances within the orbit of Mercury. While the first confirmed interstellar object, 'Oumuamua, has unclear composition and origin, future interstellar visitors have the potential to shed light on this mystery, especially if they happen to pass near the sun. Experience with past Sungrazers suggests that discovery from the ground is a crucial component to obtaining compositional information about the deep interior of the object's nucleus, so LSST will likely prove crucial in this regard. Among known comets that have passed close to the sun, none are particularly likely to have been extrasolar in origin, and hence our observations of these comets sheds little light on the question of 'Oumuamua's composition. Nonetheless, we expect that perhaps one of these comets may in fact be interstellar in origin. Future spectroscopy of the gas evaporated from such comets could shed new light on the nurseries of the large-than-expected population of 'Oumuamua-like objects.

#### ACKNOWLEDGEMENTS

The authors would like to thank John Raymond for helpful conversations. We made use of NASA's ADS, JPL's small-body database, and the arXiv. JCF is supported by an ITC Fellowship, and this work was supported in part by a grant from the Breakthrough Prize

Foundation.

## REFERENCES

- A'Hearn M. F., Millis R. C., Schleicher D. O., Osip D. J., Birch P. V., 1995, *Icarus*, 118, 223
- Anderson E., Francis C., 2012, *Astronomy Letters*, 38, 331
- Bialy S., Loeb A., 2018, *The Astrophysical Journal Letters*, 868, L1
- Bland-Hawthorn J., Gerhard O., 2016, *Annual Review of Astronomy and Astrophysics*, 54, 529
- Bolin B. T. et al., 2018, *The Astrophysical Journal Letters*, 852, L2
- Brown J. C., Carlson R. W., Toner M. P., 2015, *The Astrophysical Journal*, 807, 165
- Brown J. C., Potts H. E., Porter L. J., Le Chat G., 2011, *Astronomy and Astrophysics*, 535, A71
- Bryans P., Pesnell W. D., 2012, *The Astrophysical Journal*, 760, 18
- Bryans P., Pesnell W. D., 2016, *The Astrophysical Journal*, 822, 77
- de la Fuente Marcos C., de la Fuente Marcos R., Aarseth S. J., 2018, *Monthly Notices of the Royal Astronomical Society*, 476, L1
- Do A., Tucker M. A., Tonry J., 2018, *The Astrophysical Journal Letters*, 855, L10
- Downs C., Linker J. A., Mikić Z., Riley P., Schrijver C. J., Saint-Hilaire P., 2013, *Science*, 340, 1196
- Fernández J. A., Sosa A., 2012, *Monthly Notices of the Royal Astronomical Society*, 423, 1674
- Fink U., 2009, *Icarus*, 201, 311
- Hein A. M., Perakis N., Eubanks T. M., Hibberd A., Crowl A., Hayward K., Kennedy III R. G., Osborne R., 2017, arXiv e-prints, 1711, arXiv:1711.03155
- Hughes D. W., 1988, *Icarus*, 73, 149
- Jones G. H. et al., 2018, *Space Science Reviews*, 214, 20
- Knight M. M., A'Hearn M. F., Biesecker D. A., Faury G., Hamilton D. P., Lamy P., Llebaria A., 2010, *The Astronomical Journal*, 139, 926
- Kohl J. L. et al., 1995, *Solar Physics*, 162, 313
- Kreutz H. C. F., 1888, *Untersuchungen Über Das Comentesystem* 1843 I, 1880 I Und 1882 II.
- Langland-Shula L. E., Smith G. H., 2007, *The Astrophysical Journal Letters*, 664, L119
- Langland-Shula L. E., Smith G. H., 2011, *Icarus*, 213, 280
- Laughlin G., Batygin K., 2017, *Research Notes of the American Astronomical Society*, 1, 43
- Lemen J. R. et al., 2012, *Solar Physics*, 275, 17
- Levison H. F., 1996, in *Completing the Inventory of the Solar System*. pp 173–191
- Lingam M., Loeb A., 2018, *The Astronomical Journal*, 156, 193
- Mamajek E., 2017, *Research Notes of the American Astronomical Society*, 1, 21
- Meech K. J. et al., 2017, *Nature*, 552, 378
- Micheli M. et al., 2018, *Nature*, 559, 223
- Moro-Martín A., Turner E. L., Loeb A., 2009, *The Astrophysical Journal*, 704, 733
- Nordström B. et al., 2004, *Astronomy and Astrophysics*, 418, 989
- Pesnell W. D., Bryans P., 2014, *The Astrophysical Journal*, 785, 50
- Rafikov R. R., 2018a, arXiv e-prints, 1809, arXiv:1809.05133
- Rafikov R. R., 2018b, *The Astrophysical Journal Letters*, 867, L17
- Raymond J. C., Downs C., Knight M. M., Battams K., Giordano S., Rosati R., 2018, *The Astrophysical Journal*, 858
- Raymond J. C., McCauley P. I., Cranmer S. R., Downs C., 2014, *The Astrophysical Journal*, 788, 152
- Reid I. N., Gizis J. E., Hawley S. L., 2002, *The Astronomical Journal*, 124, 2721
- Schleicher D. G., 2008, *The Astronomical Journal*, 136, 2204
- Schrijver C. J., Brown J. C., Battams K., Saint-Hilaire P., Liu W., Hudson H., Pesnell W. D., 2012, *Science*, 335, 324
- Schwamb M. E. et al., 2018, arXiv e-prints, 1802, arXiv:1802.01783
- Sekanina Z., Kracht R., 2018, arXiv e-prints, 1812, arXiv:1812.07054
- Seligman D., Laughlin G., 2018, *The Astronomical Journal*, 155, 217
- Siraj A., Loeb A., 2018, arXiv e-prints, 1811, arXiv:1811.09632
- Trick W. H., Coronado J., Rix H.-W., 2018, arXiv e-prints, 1805, arXiv:1805.03653
- Trilling D. E. et al., 2018, *The Astronomical Journal*, 156, 261
- Weissman P. R., Lowry S. C., 2001, in *Bulletin of the American Astronomical Society*. p. 31.04
- Ye Q.-Z., Hui M.-T., Kracht R., Wiegert P. A., 2014, *The Astrophysical Journal*, 796, 83